Peculiarities of the adsorption kinetics of mixed convex plus concave contour objects

Pradip B. Shelke,[1,2] S. B. Ogale,[3] M. D. Khandkar,[4,*] and A. V. Limaye[1]
[1]*Center for Advanced Studies in Materials Science and Solid State Physics, Department of Physics, University of Pune, Pune 411 007, India*
[2]*Department of Physics, Ahmednagar College, Ahmednagar 414 001, India*
[3]*Physical and Materials Chemistry Division, National Chemical Laboratory, Dr. Homi Bhabha Road, Pune 411 008, India*
[4]*Department of Physics, Kishinchand Chellaram College, Mumbai 400 020, India*
(Received 7 January 2008; published 19 June 2008)

Random sequential adsorption of mixed convex plus concave contour (MC) objects exhibits some distinctly different peculiar characteristics than the cases of purely convex objects. Though the substrate coverage approaches the jamming limit with time t as t^{-p}, same as that for convex objects, the law $p \sim 1/d_f$, valid for convex objects with d_f degrees of freedom, does not hold for MC objects. Interestingly, for a fixed number of degrees of freedom, the exponent p changes with the degree of nonconvexity and bears a near perfect correlation with the same.

DOI: 10.1103/PhysRevE.77.066111 PACS number(s): 82.20.Wt, 47.63.mh, 68.43.Mn, 89.75.Fb

The study of the adsorption of objects on surfaces is clearly of great significance and relevance to a wide variety of deposition processes in real physical, chemical, and biological systems. The adsorbing entities in these systems come in a wide variety of geometries, dimensionalities, sizes, and shapes. Correspondingly, their adsorption kinetics can be expected to exhibit a rich structure in space time. From the theoretical standpoint, however, it is important to explore whether some generic system can be developed which may not depend on the object details. In the case of the most widely studied random sequential adsorption (RSA) of two-dimensional (2D) objects, such a system is known to occur for convex contoured objects in the form of power law approach to the so-called jamming limit and the inverse dependence of the exponent on the degrees of freedom of the object. Unfortunately, in spite of the existence of several objects and adsorption situations [1] of interest in the domain of mixed concave plus convex contoured (MC) objects, to the best of our knowledge no work has been devoted to such cases. In this work we demonstrate that the mixed contour character of the object shape renders different features to the adsorption kinetics wherein the degree of non-convexity plays a key role. The broad applicability of these results in various applications is also demonstrated by consideration of one particular example of current interest, namely delivery of drugs using mixed contour nanoparticles.

In the RSA model [2], particles are added randomly and sequentially on a substrate without overlapping each other. In the case of RSA of finite area objects on a continuum substrate, the adsorbed objects occupy some area on the substrate and cause blocking of the area available for new additions, limiting the value of substrate coverage to $\Theta(\infty)$, called jamming coverage. In general, the approach of instantaneous coverage $\Theta(t)$ to $\Theta(\infty)$ is found to be a power law $\Theta(\infty)-\Theta(t) \sim t^{-p}$. Feder [3] pointed out that the exponent p takes the value 1/2 in the case of RSA of 2D circular disks and suggested $p=1/d$, for a d-dimensional disk on a 2D continuum substrate. Later, Swendsen [4] showed that the same relation should also hold for the RSA of objects of arbitrary shape, provided that the objects are dropped with random orientations. However, P. Viot and G. Tarjus [5] found that the Swendsen conjuncture $p=1/d$ is not true and stated the relation $p=1/d_f$, d_f being the degrees of freedom of the adsorbing object. RSA of squares, rectangles, strongly elongated ellipses and spherocylinders have led to a value of exponent of 1/3 within statistical uncertainties [6] which validates the relation $p=1/d_f$. However, it is important to observe that all the objects for which the simulations are carried out thus far are purely convex in shape. To the best of our knowledge there are no reports on RSA of MC objects. In one of our earlier studies [7], we established the universal behavior of the power law approach to the jammed state irrespective of object types. Hence, even for MC objects a power law behavior can be expected. However, in another work [8] on RSA of angled objects we showed that the RSA dynamics gets drastically altered for slightest increase in the angle from the value zero (for the case of needles), and this has its origin in the qualitative change taking place in the object shape from needle to the angled object. Since MC objects have qualitatively different shapes than the convex objects, it becomes important to explore the validity of $p=1/d_f$ for MC objects.

We have carried out a computer simulation study of RSA of a specific object type, namely, a coupled three-circle object which is MC in nature. It consists of three circular disks, of the same radius r, where two disks touch the central one and subtend an angle θ at the center of the central disk. In computer simulation on a plane continuum substrate of size $A=L\times L$, at each time step one object with random position and orientation is tried for adsorption. The object is successfully adsorbed if it does not overlap with previously adsorbed ones, otherwise it is rejected. In either case the time is incremented by one unit. For a fixed value of object area $a=3\pi r^2$, simulations were carried out for various values of θ, ranging from 60° to 180°. For each case the simulations are carried out up to 2×10^8 time steps and the results are obtained by averaging over 10 simulation runs. The a/A ratio is

*Present address: Laboratory of Physics, Helsinki University of Technology, P.O. Box 1100, FIN-02015 TKK, Finland

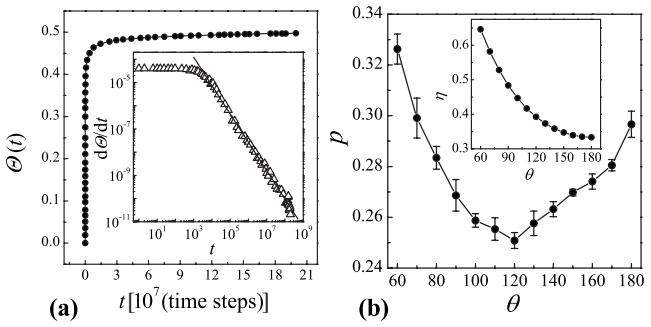

FIG. 1. (a) Plot of $\Theta(t)$ vs t for coupled three-circle object with $\theta=120°$. Inset shows the plot of $d\Theta(t)/dt$ versus t on a log-log scale. (b) Variation of exponent p and packing efficiency factor η (inset) for different θ values (in degrees).

kept low (=0.00004) enough to minimize the finite size effects. Also, periodic boundary conditions are employed to eliminate boundary effects.

Figure 1(a) shows a representative graph of coverage $\Theta(t)$ versus t for an object with $\theta=120°$. Inset shows $d\Theta(t)/dt$ versus t plot on a log-log scale. The linear nature of the graph in the asymptotic regime confirms that the kinetics of adsorption follows the law, $\Theta(\infty)-\Theta(t)\sim t^{-p}$. The slope of the best-fit line in the asymptotic time regime gives the value of the exponent when equated to $-(p+1)$. Interestingly, the exponent p shows a nonmonotonic dependence on the subtended angle θ [Fig. 1(b)]. The value of p goes on decreasing gradually as θ increases from 60° to 120°, and after bottoming out there it rises gradually as θ increases. More importantly, it clearly establishes that the relation $p=1/d_f$, which is valid for convex objects, is defined for MC objects such as coupled three-circle objects ($d_f=3$) as the obtained p values are significantly different from 1/3. The cause for this deviation and the system involved needs to be investigated by looking into various aspects.

To explain the variation of saturation coverage with aspect ratio in the case of the RSA of rectangular objects, Vigil and Ziff [9] introduced a factor η called "packing efficiency factor," given by the ratio of the actual area covered by the object to the area swept by the object in complete rotation. For coupled three-circle objects, it is observed that η goes on falling monotonically with increasing θ [inset of Fig. 1(b)]. Hence the peculiar nonmonotonic dependence of the exponent p on the variable θ observed for MC objects cannot be explained by the consideration of the packing efficiency η alone. It is then instructive to compare the adsorption of MC versus convex bodies in some depth.

Let us first discuss the adsorption of convex bodies. In the case of hard disks it was first conjectured by Feder [3] and later proved by Swendsen [4] that the coverage follows the law $\Theta(\infty)-\Theta(t)\sim t^{-\alpha}$ with $\alpha=1/2$. Their analysis was based on the exclusion of an area of radius $2r$ around each disk of radius r for selecting the center of a newly arriving disk. After a certain time t_c characterizing the beginning of the asymptotic regime, the area that is available to the center of a new disk consists of isolated targets: small disconnected areas that can be occupied by only one additional disk [Fig. 2(a)]. For a typical target, having linear size h at instant

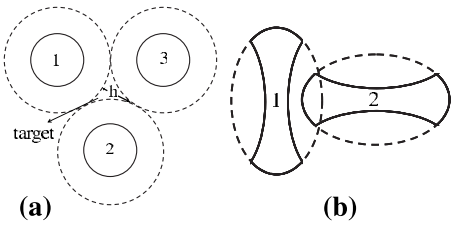

FIG. 2. (a) Target area excluded by circular disks. (b) In the vicinity of each other the MC objects (solid line) get adsorbed without overlap while the corresponding convex objects (dotted line) overlap with each other.

t, the area available for the disk getting newly added goes as h^2. Thus the rate of disappearance of such a target is proportional to h^2 and hence number density $n(h,t)$ of targets of linear size h at instant t decays as $n(h,t)\approx n(h,t_c)e^{-kh^2(t-t_c)}$. It has been further assumed that the density of targets $n(h,t_c)$ becomes a nonzero constant $n(0,t_c)$, when h goes to zero. This then leads to a power law $\rho(\infty)-\rho(t)=\int_0^{h_c}dh\, n(h,t)\sim t^{-1/2}$, in the asymptotic time regime, here $\rho(\infty)$ and $\rho(t)$ are jamming and instantaneous number densities. For elongated objects such as ellipse, Talbot *et al.* [10] argued that the rate of disappearance of the targets has to be proportional to h^3 instead of h^2 because of extra factor h arising from orientational restrictions to explain the observed power law $\rho(\infty)-\rho(t)=t^{-1/3}$. For objects with even more complicated shapes the nature of the targets will be equally complex, hence we extended these arguments [7] by assuming that the probability of disappearance of a target is proportional to h^α and the density of targets $n(h,t_c)$ becomes $h^{-1+\beta}$ when h becomes zero, where α and β are real positive numbers. With these assumptions, RSA dynamics is observed to follow power law $\rho(\infty)-\rho(t)\sim(t)^{-p}$ in the asymptotic regime, with $p=\beta/\alpha$. In this study we also revealed the crucial role of the distribution of the density of targets at time t_c in the RSA dynamics.

Now consider the case of adsorption of an MC object (solid line) as shown in Figure 2(b). It shows a newly adsorbing object 2 in the vicinity of an already adsorbed object 1, both derived from the corresponding convex bodies (dotted line). It is clear from the figure that in such instances the adsorption in the vicinity of the already adsorbed object which meets failure in the case of a convex object, succeeds in the case of an MC object. This brings in the crucial role of the nonconvex nature of the object in the adsorption process. Thus, in the initial time regime, some of the failed adsorption attempts in the case of convex objects will be successful in the case of MC objects. These will eventually result in a configuration where the adsorbed objects will have a closer proximity in the case of MC objects as compared to that in the case of convex objects. Therefore, after a characteristic time t_c, the nature of the isolated targets in the case of MC objects will be such that there will be more stringent conditions (higher value of α) on orientations of the newly adsorbing object to become successfully adsorbed. Also, due to the close proximity of adsorbed objects in the case of MC objects, the weight of the number of smaller size targets in the distribution of targets will be more in the case of MC objects.

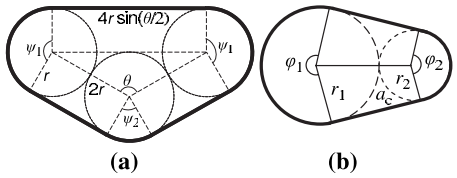

FIG. 3. Convex shape (thick solid line) of minimum area for coupled (a) three-circle and (b) two-circle objects.

This fact leads to a lowering of the value of β since $n(h,t_c) \sim h^{-(1-\beta)}$. As a result, the exponent $p=\beta/\alpha$ will become lower in the case of MC objects than that for convex objects. This discussion suggests the greater the departure from the convexity, the more likely is its influence on the value of the exponent p. The coupled three-circle objects with $\theta=60°$ and 180° are very close to convex shapes, viz. an equilateral triangle and a rectangle, respectively, while the appearance of an object with $\theta=120°$ is far from any convex shape. The above discussion then qualitatively explains why the exponent in the case of $\theta=120°$ is significantly lower than that for $\theta=60°$ or 180°.

To explore how good the correlation is between the exponent p and the departure from convexity, we now quantify the degree of nonconvexity by defining the "coefficient of departure from convexity," δ. We consider the closest convex shape of minimum area which circumscribes the coupled three-circle object, as shown in Fig. 3(a). We then define δ as the difference in the area of coupled three-circle object and the area of the circumscribing convex shape per unit area of the coupled three-circle object, i.e.,

$$\delta(\theta) = \left(a - \left[4r^2 + 4r^2 \sin(\theta/2) + 4r^2 \sin(\theta/2)\cos(\theta/2) + r^2\psi_1 + \frac{1}{2}r^2\psi_2 \right] \right) \Big/ a$$

where $\psi_1=(\pi+\theta)/2$ and $\psi_2=\pi-\theta$.

The graphs of the coefficient of departure from convexity δ and the exponent p for the coupled three-circle objects with different θ values are shown in Fig. 4(a). The two curves show an excellent overlap, implying a near perfect correlation between the plotted quantities, especially for θ values less than 160°. For $\theta \geq 160°$, although the correlation is slightly weak, both the quantities follow the same trend. The value $r_{\delta p}=0.99$, of correlation coefficient for $\theta<160°$, indicates the near perfect positive correlation between δ and p. Thus, the greater the magnitude of the coefficient of departure from convexity ($|\delta|$), the less is the value of the exponent and hence the deviation of the exponent from 1/3 is greater, i.e., $1/d_f$.

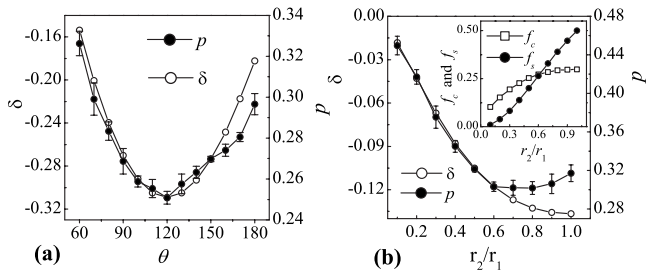

FIG. 4. (a) Coefficient of departure from convexity δ and exponent p as a function of θ (in degrees) for a coupled three-circle object. (b) Coefficient of departure from convexity δ and exponent p as a function of r_2/r_1 for a coupled two-circle object. Inset shows f_c and f_s vs r_2/r_1.

To ensure that the observations discussed above are not object specific, we also carried out similar studies for another type of an MC object, namely, a coupled two-circle object comprising two touching circles of radii r_1 and r_2. For a fixed value of object area $a=\pi(r_1^2+r_2^2)$, the same simulation procedure of RSA of coupled three-circle objects is carried out for various values of r_2/r_1 ranging from 0.1 to 1. Here also we define δ as

$$\delta(r_2/r_1) = \left(a - \left[(r_1+r_2)\sqrt{(r_1+r_2)^2-(r_1-r_2)^2} + \frac{1}{2}(\phi_1 r_1^2 + \phi_2 r_2^2) \right] \right) \Big/ a$$

[see Fig. 3(b)].

In Fig. 4(b) we present the plots of the δ and p as a function of r_2/r_1. Here again, an excellent overlap of the two plots, especially for r_2/r_1 less than or equal to 0.6, establishes that the coefficient of departure from convexity and the exponent are strongly correlated. Here also the value of $r_{\delta p}=1$ for $r_2/r_1 \leq 0.6$ indicates the perfect positive correlation between δ and p in this range of radius ratio. The correlation is relatively weak when $r_2/r_1>0.6$. This can be understood as follows: As stated earlier, the different behavior shown by the MC objects has its origin in their possibility of begin adsorbed with some of their parts in the crevices. In the case of coupled two-circle objects, with change in the radius ratio, not only does the degree of nonconvexity change, but there is also a change in the size of the circles. Hence the effect of this obviously depends on the area of the crevice, a_c [shown in Fig. 3(b)] against that of smaller circle, a_s. The normalized fractions $f_c=a_c/a$ and $f_s=a_s/a$ of these areas as a function of radius ratio r_2/r_1 are shown as an inset in Fig. 4(b). The plot shows that there is a crossover between them beyond radius ratio 0.6. Beyond this radius ratio, the role of crevices becomes less significant and the object starts behaving as if it is a convex object and the exponent tends to approach to value 1/3.

To illustrate broad applicability and implications of our results to various adsorption systems, here we discuss an issue of immense interest, namely the targeted drug delivery. In this process, the drug carrying nanoparticles circulate through the blood system and get adsorbed on the desired tissue. But during such circulation, macrophages treat these particles as foreign objects, engulfing and removing (phagocytosis) them from the blood system. Champion and Mitragotri [11] have shown that the ability of macrophages to engulf a particle depends sensitively on the particle shape, wherein it is observed that the particle shapes having sudden change in curvature cannot be phagocytosed easily. Taking into account these aspects, Champion *et al.* [12] also have

TABLE I. Time to attain 40% coverage and exponent p values for various object shapes.

Object shape	Time (simulation steps) to attain 40% coverage	Time (simulation steps) to attain 49% coverage	Exponent p
Circular disk	$5.8\times10^4\pm2.0\times10^3$	$4.3\times10^5\pm1.3\times10^4$	0.50 ± 0.02
Coupled two-circle object with radius ratio 1	$1.48\times10^5\pm5.0\times10^3$	$4.0\times10^6\pm2.0\times10^5$	0.32 ± 0.01
Coupled three-circle object with $\theta=60°$	$1.57\times10^5\pm4.0\times10^3$	$1.0\times10^7\pm6.0\times10^5$	0.33 ± 0.01
Coupled three-circle object with $\theta=180°$	$3.9\times10^5\pm1.3\times10^4$	$1.0\times10^8\pm2.0\times10^7$	0.30 ± 0.01
Coupled three-circle object with $\theta=120°$	$4.6\times10^5\pm2.5\times10^4$	$1.0\times10^8\pm1.0\times10^7$	0.25 ± 0.01

engineered a variety of shapes, many of which are flat and mixed contoured, to evade the phagocytosis in drug delivery.

Clearly, the effectiveness of drug delivery to the desired tissue using such MC nanoparticles will depend on both the rate of adsorption and the total amount of adsorbed particles. Interestingly, the saturation coverage, i.e., the total amount adsorbed in infinite time, is almost insensitive to the object shape. For instance, for coupled three-circle objects, the values are within the range 0.50 to 0.52 for different values of θ, and for coupled two-circle objects, they are in the range 0.53 to 0.54 which are close to that for convex objects [6]. However, knowing that the real process does not run for infinite time, what is more important is the time taken to attain specific substrate coverage. For example, for a fixed value of ratio of object area to substrate area, the average time required for attaining certain substrate coverage, say 40% and 49%, for a few representative objects along with their exponent p values are given in Table I. One can immediately notice that in both 40% and 49% coverage cases, the time in the case of circular disks is significantly lower. However, it should also be borne in mind that a circular shape is most susceptible to phagocytosis. Also, one can immediately notice that the objects with a higher exponent p value require less time to attain the required coverage.

One comment is in order: The reason behind choosing the coverage values 40% and 49% is that the time taken to reach these coverages is well beyond t_c and hence it is reasonable to correlate these times with the exponent p, characteristic of asymptotic regime kinetics, which is the subject of the present study. However, it also should be noted that t^{-p} kinetics applies strictly to the asymptotic regime and one should generate approximate interpolants valid for any time by combining the asymptotic expression with low coverage series expansion, similar to that by Dickman *et al.* [13], or virial-like expansion described by Ricci *et al.* [14], especially for low coverage cases. Any studies in this direction will be interesting and may be more relevant to drug delivery application.

The point which we would like to stress is that there is clearly some optimum shape for the drug carrying particle that is a compromise between nonsphericity in general and nonconvexity in particular, which is good for avoiding phagocytosis and sphericity or convexity which is good for rapid adsorption. In conclusion, in the case of RSA of mixed contour objects, the law $p\sim1/d_f$ is not applicable. The exponent p in the adsorption kinetics is found to depend on the degree of departure of the object shape from convexity and bears a near perfect correlation with the same. Most importantly, the time taken to build a specific surface coverage is found to depend on the object shape and its degree of nonconvexity. These behaviors are distinctly different as compared to the well studied cases of purely convex contoured objects.

P.B.S. and A.V.L. acknowledge the University of Pune and S.B.O. acknowledges DST, for funding.

[1] N. Saettel *et al.*, J. Mater. Chem. **15**, 3175 (2005); Maya Schock *et al.*, J. Phys. Chem. B **110**, 12835 (2006); Norihiro Mizoshita and Takahiro Seki, Soft Matter **2**, 157 (2006).

[2] J.W. Evans, Rev. Mod. Phys. **65**, 1281 (1993); J.-S. Wang and R. B. Pandey, Phys. Rev. Lett. **77**, 1773 (1996); J. Talbot *et al.*, Colloids Surf., A **165**, 287 (2000).

[3] J. Feder, J. Theor. Biol. **87**, 237 (1980).

[4] R. H. Swendsen, Phys. Rev. A **24**, 504 (1981).

[5] P. Viot and G. Tarjus, Europhys. Lett. **13**, 295 (1990).

[6] Viot *et al.*, J. Chem. Phys. **97**, 5212 (1992).

[7] P. B. Shelke, M. D. Khandkar, A. G. Banpurkar, S. B. Ogale, and A. V. Limaye, Phys. Rev. E **75**, 060601(R) (2007).
[8] M. D. Khandkar, A. V. Limaye, and S. B. Ogale, Phys. Rev. Lett. **84**, 570 (2000).
[9] R. D. Vigil and R. M. Ziff, J. Chem. Phys. **91**, 2599 (1989).
[10] J. Talbot, G. Tarjus, and P. Schaaf, Phys. Rev. A **40**, 4808 (1989).
[11] J. Champion and S. Mitragotri, Proc. Natl. Acad. Sci. U.S.A. **103**, 4930 (2006).
[12] J. Champion, Y. Katare, and S. Mitragotri, Proc. Natl. Acad. Sci. U.S.A. **104**, 11901 (2007).
[13] R. Dickman, J. Wang, and I. Jensen, J. Chem. Phys. **94**, 8252 (1991).
[14] S. Ricci *et al.*, J. Chem. Phys. **97**, 5219 (1992).